Available online at www.sciencedirect.com

ScienceDirect

Procedia Structural Integrity 46 (2023) 80–86

Structural Integrity Procedia

www.elsevier.com/locate/procedia

5th International Conference on Structural Integrity and Durability, ICSID 2021

Fatigue crack prediction in ceramic material and its porous media by using peridynamics

Cong Tien Nguyen[a], Selda Oterkus[a]*, Erkan Oterkus[a], Islam Amin[a,b], Murat Ozdemir[a,c], Abdel-Hameed El-Aassar[d], Hosam Shawky[d]

[a]*PeriDynamics Research Centre (PDRC), Department of Naval Architecture, Ocean and Marine Engineering, University of Strathclyde, Glasgow, G4 0LZ, UK*

[b]*Department of Naval Architecture and Marine Engineering, Port Said University, Port Said, Egypt*

[c] *Faculty of Marine Science, Ordu University, Ordu, Turkey*

[d] *Egypt Desalination Research Centre of Excellence (EDRC) and Hydrogeochemistry Department, Desert Research Centre, Cairo, Egypt*

Abstract

Peridynamics is a nonlocal reformulation of the classical continuum mechanics using integro-differential equations. Since the integro-differential equations used in peridynamics are valid in both continuous and discontinuous models, the theory is suitable for predicting progressive damages. In this study, fatigue crack growth in a ceramic material and its porous media is predicted by using the peridynamic model for fatigue cracking. First, the fatigue crack propagation in compact specimen of a non-porous ceramic material is considered. The predicted fatigue crack growth rate is compared with experimental results. Next, the fatigue crack growths in ceramic material with different porosity levels are investigated. The fatigue crack growth rate of porous materials is compared with the non-porous material to analyse the effects of porosity on fatigue crack growth. A linear relation between the relative change of fatigue crack growth rate, stress intensity factor range and porosity level is obtained by using linear regression analysis.

© 2023 The Authors. Published by Elsevier B.V.
This is an open access article under the CC BY-NC-ND license (https://creativecommons.org/licenses/by-nc-nd/4.0)
Peer-review under responsibility of ICSID 2021 Organizers

Keywords: Fatigue crack growth; Ceramic; Porosity; Porous media; Peridynamics

* Corresponding author. Tel.: +44-141-548-4979.
E-mail address: selda.oterkus@strath.ac.uk, nguyen-tien-cong@strath.ac.uk

2452-3216 © 2023 The Authors. Published by ELSEVIER B.V.
This is an open access article under the CC BY-NC-ND license (https://creativecommons.org/licenses/by-nc-nd/4.0)
Peer-review under responsibility of ICSID 2021 Organizers
10.1016/j.prostr.2023.06.014

1. Introduction

Ceramic materials often have high hardness, high melting point, low mass density. Therefore, they can be used in many applications for high temperature environments. Moreover, since ceramics are resistant to abrasion and have high chemical resistance, its applications for corrosive environments such as ceramic water filtration and purification membranes in wastewater treatment processes are growing in popularity. Ceramics also can enable a wider range of clean-in-place options such as using harsh chemicals or high pressure from two directions. Additionally, the ceramic membranes can be specified to highly complex geometries and tight tolerances, facilitating more flexible designs that make filtration modules more energy efficient.

Under cyclic loading conditions such as vibrations or cyclic thermal loads, ceramic materials can experience fatigue damages which are often high cycle fatigue phenomena with zero ductility. To predict fatigue crack propagation, traditional numerical methods such as the finite element method or various modified versions of finite element method need to use additional criteria to predict crack growth speed and direction. By contrast, peridynamics is a reformulation of classical continuum mechanics by using integro-differential equations (Silling, 2000). Since the integro-differential equations used in peridynamics are valid in both continuous and discontinuous models, the theory is suitable for predicting progressive damages even for crack branching and multiple cracks phenomena (Madenci and Oterkus, 2014).

For high cycle fatigue damage prediction, Silling and Askari (2014) developed a peridynamic model for fatigue cracking based on the cyclic bond strain range. This peridynamic fatigue model was applied and validated by Zhang et al. (2016) and Jung and Seok (2017). Later, Nguyen et al. (2021) further extended the capability of the peridynamic fatigue model by considering effects of overloads and underloads. The authors modified peridynamic fatigue equations by introducing the retardation factor based on modified Wheeler models. Nguyen et al. (2020) also developed an energy-based peridynamic fatigue model using cyclic bond energy release rate range.

In this study, fatigue crack growth in a ceramic material and its porous media is predicted by using the peridynamic fatigue model developed by Silling and Askari (2014). First, a brief review of the peridynamic fatigue model is given in Section 2. In Section 3, fatigue crack propagation in compact specimens of a Magnesia-Partially-Stabilized Zirconia ceramic material is predicted and compared with experimental results. Moreover, fatigue crack growths on the ceramic material with different porosity levels are also predicted and compared with the fatigue crack growth on non-porous material. Finally, a conclusion is given in Section 4.

2. Peridynamic fatigue model

In peridynamics, a material point has interactions with its family members which are the surrounding material points located within a distance, δ. The finite distance δ is called the horizon size. The interaction between two material points is called a bond. The equation of motion for one material point in peridynamics can be expressed in either the integro-differential or discrete equations as (Silling and Askari, 2005, Madenci and Oterkus, 2014)

$$\rho(\boldsymbol{x})\ddot{\boldsymbol{u}}(\boldsymbol{x},t) = \int_{H_x} \psi(\boldsymbol{x}'-\boldsymbol{x},t)\left(\boldsymbol{t}(\boldsymbol{u}'-\boldsymbol{u},\boldsymbol{x}'-\boldsymbol{x},t) - \boldsymbol{t}'(\boldsymbol{u}-\boldsymbol{u}',\boldsymbol{x}-\boldsymbol{x}',t)\right)dV' + \boldsymbol{b}(\boldsymbol{x},t) \tag{1a}$$

or

$$\rho_{(k)}\ddot{\mathbf{u}}_{(k)} = \sum_{j=1}^{N_k} \psi_{(k)(j)}\left(\mathbf{t}_{(k)(j)} - \mathbf{t}_{(j)(k)}\right)V_{(j)} + \mathbf{b}_{(k)} \tag{1b}$$

where ρ and $\ddot{\mathbf{u}}$ represent the mass density and acceleration, and $\mathbf{b}$ represents the external body force density. The parameter N_k represents the number of family members of the material point k. The term $V_{(j)}$ is the volume of the material point j which is a family member of the material point k. The term $\mathbf{t}_{(k)(j)}$ denotes the force density that the material point j exerts on the material point k and $\mathbf{t}_{(j)(k)}$ corresponds to the force density that material point k exerts

on the material point j. The parameter $\psi_{(k)(j)}$ determines whether the interaction is intact or broken and it can be defined as (Silling and Askari, 2005)

$$\psi_{(k)(j)}\left(\boldsymbol{x}_{(j)}-\boldsymbol{x}_{(k)},t\right)=\begin{cases}1 & \text{if an intact interaction exists,}\\ 0 & \text{otherwise.}\end{cases} \tag{2}$$

Since the equations of motion given in Eq. (1) does not include partial derivatives, these equations exist in both continuous and discontinuous models. Therefore, peridynamics is well suitable for predictions of progressive damages. In peridynamics, the damage index, φ is used to represent the local damages on the structure. This damage index is the ratio of broken interactions to the total number of interactions within the horizon of a material point, which can be represented as (Silling and Askari, 2005)

$$\varphi\left(\boldsymbol{x}_{(k)},t\right)=1-\frac{\sum_{j=1}^{N_k}\psi_{(k)(j)}\left(\boldsymbol{x}_{(j)}-\boldsymbol{x}_{(k)},t\right)V_{(j)}}{\sum_{j=1}^{N}V_{(j)}} \tag{3}$$

In peridynamic fatigue model (Silling and Askari, 2014), each interaction (bond) has a remaining life, λ. A bond with the remaining life of $0<\lambda\leq 1$ is considered as intact. Meanwhile, a bond with the remaining life of $\lambda=0$ is considered as broken. The peridynamic fatigue model (Silling and Askari, 2014) includes equations for fatigue crack initiation (phase I) and fatigue crack growth (phase II). The fatigue equation for phase I is based on the $\varepsilon-N$ curve. Meanwhile, the fatigue equation for phase II is based on the Paris' law. The fatigue equation for phase II can be represented as

$$\lambda_{(k)(j)}^{(0)}=1,\lambda_{(k)(j)}^{(N)}=\lambda_{(k)(j)}^{(N-1)}-A_2\left(\varepsilon_{(k)(j)}^{(N)}\right)^{m_2}\ \text{with}\ A_2>0,m_2>0 \tag{4a}$$

with

$$\varepsilon_{(k)(j)}^{(N)}=\left|s_{(k)(j)}^{(N+)}-s_{(k)(j)}^{(N-)}\right|=\left|s_{(k)(j)}^{(N+)}(1-R)\right| \tag{4b}$$

where $\lambda_{(k)(j)}^{(N)}$ and $\varepsilon_{(k)(j)}^{(N)}$ represent the fatigue life and cyclic bond strain range of this interaction at N^{th} cycle. The parameters $s_{(k)(j)}^{(N+)}$ and $s_{(k)(j)}^{(N-)}$ are bond stretches corresponding to maximum loading and minimum loading at N^{th} cycle, respectively. The parameters A_2 and m_2 are fatigue parameters for phase II. These parameters can be calibrated from experimental results (Silling and Askari, 2014). The parameter R in Eq. (4b) represents the loading ratio.

Beyond phase II (the fatigue crack growth phase), structures can experience rapid crack growth (phase III) which can be predicted by using the traditional peridynamic model (Silling and Askari, 2005, Madenci and Oterkus, 2014). Therefore, the interaction state of a bond can be defined as

$$\begin{cases}\lambda_{(k)(j)}^{(N)}\leq 0 \quad \text{or} \quad s_{(k)(j)}\geq s_c \ \rightarrow\ \psi_{(k)(j)}=0\\ \lambda_{(k)(j)}^{(N)}>0 \quad \text{and} \quad s_{(k)(j)}<s_c \ \rightarrow\ \psi_{(k)(j)}=1\end{cases} \tag{5}$$

where s_c represents the critical bond stretch (Silling and Askari, 2005, Madenci and Oterkus, 2014).

3. Numerical results

In this section, first, the fatigue crack growth on a single edge-notch ceramic plate subjected to cyclic loading is predicted in Section 3.1. Next, the fatigue crack growths for ceramic plates with different porosity levels are predicted in Section 3.2. Finally, the fatigue crack growth for ceramic plates with variable porosity levels are predicted in Section 3.3. In all sections, the horizon size of $\delta=3.015\Delta x$ is used in peridynamic simulations (Madenci and Oterkus, 2016).

3.1. Fatigue crack growth on isotropic ceramic material

In this section, the fatigue crack growth on a single edge-notch ceramic plate subjected to cyclic loading is investigated as shown in Fig. 1. The dimensions of the plate are shown in Fig. 1(a) and the peridynamic discretized model with a mesh size of $\Delta x = W/120$ is shown in Fig. 1(b). The thickness of the plate is 3 mm and the initial crack length is $q_n = 10.2$ mm. The plate is made of Magnesia-Partially-Stabilized Zirconia Ceramic with the elastic modulus of $E = 2 \times 10^{11}$ N/m^2 and Poisson's ratio of $\nu = 0.23$ (Dauskarat et al., 1990). The plate is subjected to cyclic loading with a load range of $\Delta P = 240$ N and a load ratio of $R = 0.1$.

In peridynamics, two material points located at $(L_x, \Delta x/2)$ and $(L_x, -\Delta x/2)$, shown in pink in Fig. 1(b), are fixed to avoid rigid body motions. To apply loading conditions, material points located inside the cut-outs, shown in cyan in Fig. 1(b), are assumed as rigid with the elastic modulus of $E_{rigid} = 200E$. Meanwhile, the load $P_{max} = \Delta P/(1 - R)$ is applied to the material points located at the centers of the cut-outs as shown in red in Fig. 1(b). The fatigue parameter m_2 is chosen as $m_2 = 21$ (Dauskarat et al., 1990), meanwhile the calibrated value for parameter A_2 is obtained as $A_2 = 7.5 \times 10^{84}$.

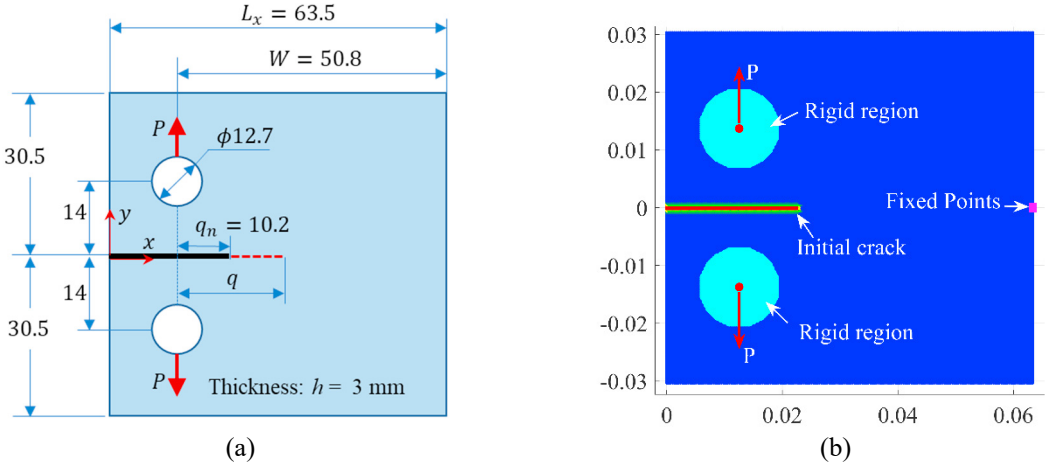

(a) (b)

Fig. 1. A single edge-notch plate (a) geometry (dimensions are in mm), (b): PD discretized model (dimensions are in m)

Fig. 2 shows the fatigue crack propagation on the plate predicted by the peridynamic fatigue model. Fig. 2(a) shows the damage on the plate at the first loading cycle where the crack length is 0.0102 m. After 4.249×10^6 cycles, the crack length is $q \approx 0.019$ m as shown in Fig. 2(b). Fig. 3 shows the crack growth $q - N$ and $dq/dN - \Delta K$ curves predicted by using peridynamic fatigue model. As shown in Fig. 3(b), the predicted $dq/dN - \Delta K$ curve agree very well with the experimental result provided by Dauskarat et al. (1990).

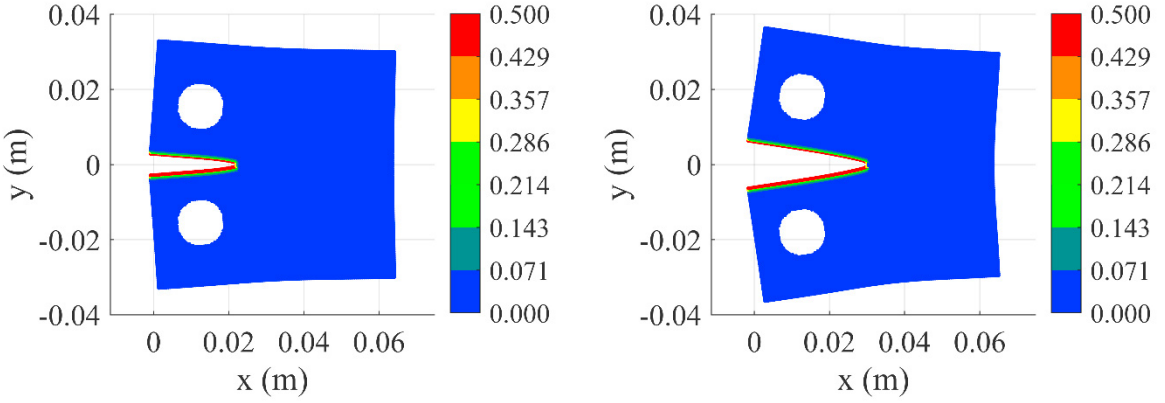

(a) (b)

Fig. 2. Fatigue damage evolution at (a) the first cycle when $q \approx 0.0102$ m, (b) 4.249×10^6 cycles when $q \approx 0.019$ m (displacements are magnified by 1000 for deformed configurations)

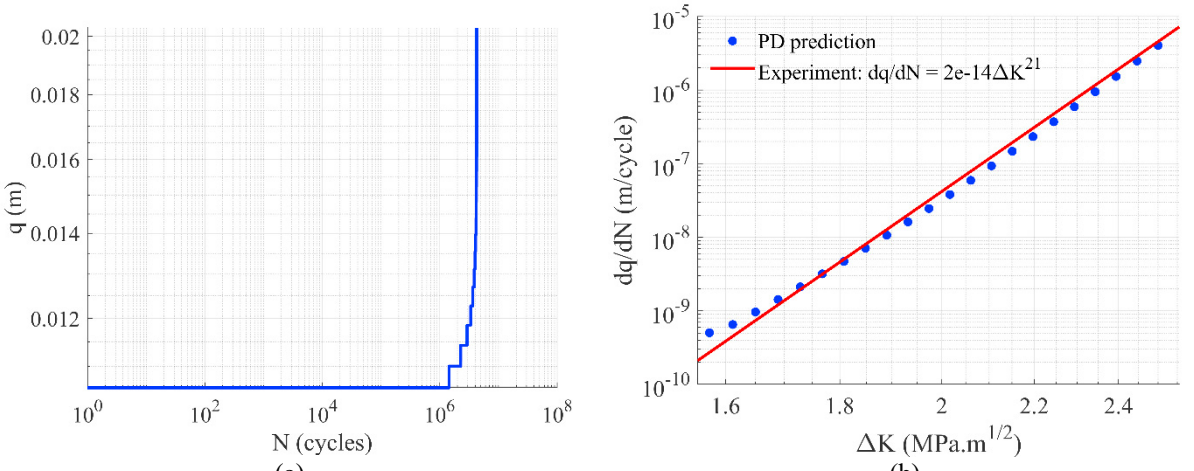

Fig. 3. Predicted fatigue crack growth (a) $q-N$ curve (b) $dq/dN-\Delta K$ curve

3.2. Fatigue crack growth on porous ceramic material

In this section, fatigue crack growth on the porous ceramic material is investigated. Specifically, the plate considered in section 3.1 is assumed to have different porosity levels as shown in Fig. 4. In discretized peridynamic model, the local porosity level for a material point is defined as

$$\phi_{(k)}\left(x_{(k)},y_{(k)}\right)=0.9\phi_0+0.2\phi_0\times r_{(k)}\left(x_{(k)},y_{(k)}\right),\ \text{with}\ 0\le r_{(k)}\left(x_{(k)},y_{(k)}\right)\le 1 \tag{6}$$

where $\phi_{(k)}\left(x_{(k)},y_{(k)}\right)$ is the local porosity at material point k, ϕ_0 is the average porosity level of the plate, $r_{(k)}\left(x_{(k)},y_{(k)}\right)$ is the random coefficient depending on location of material point k. The porosity level of each material point is represented by the reduction of its volume as

$$V_{(k)}=V_0\times\phi_{(k)}\left(x_{(k)},y_{(k)}\right)\ \text{ with }\ V_0=h\Delta x\Delta y \tag{7}$$

where V_0 represents the original volume of each material point in the discretized peridynamic model, Δx and Δy represent mesh sizes in x and y directions, respectively. The parameter h represents thickness of the plate.

As shown in Fig. 4, the ceramic plate is investigated in four different cases with the average porosity levels of $\phi_0=0.05, 0.075, 0.1$ and 0.125. By using the definition in Eq. (6), the minimum and maximum porosity levels on the plate are $0.9\phi_0$ and $1.1\phi_0$, respectively. Specifically, the porosity level on the plate in case 1 as shown in Fig. 4(a) varies from 0.045 to 0.055. Similarly, the porosity level on the plate in cases 2, 3, 4 as shown in Fig. 4(b-d) varies in the ranges $0.0675\div 0.0825$, $0.09\div 0.11$, $0.1125\div 0.1375$, respectively.

Fig. 5 shows the predicted crack growth $q-N$ and $dq/dN-\Delta K$ curves for plate with different porosity levels. As can be observed from Fig. 5(a), with the average porosity levels of $\phi_0=0.05, 0.075, 0.1$ and 0.125, the fatigue life N_f of the plate is reduced approximately $97\%, 99.14\%, 99.77\%$ and 99.93%, respectively. As can be observed from Fig. 5(b), because of porosities, the fatigue crack growth rates on the plate with porosities are significantly higher than fatigue crack growth rate on the non-porous plate. Specifically, the fatigue crack growth rate depends on the porosity level and the stress intensity factor. Therefore, to understand the relationship between the porosity level, stress intensity factor range and the fatigue crack growth rate on the plate, the relative change of logarithm of fatigue crack growth rate is defined as

$$\overline{\frac{dq}{dN}}(\phi,\Delta K)=\left[log\left(\frac{dq}{dN}(\phi,\Delta K)\right)-log\left(\frac{dq}{dN}(\phi=0,\Delta K)\right)\right]/log\left(\frac{dq}{dN}(\phi=0,\Delta K)\right) \tag{8}$$

where $\overline{\frac{dq}{dN}}(\phi, \Delta K)$ is relative change of logarithm of fatigue crack growth rate, $\frac{dq}{dN}(\phi, \Delta K)$ is the fatigue crack growth rate at stress intensity factor range of ΔK of plate with porosity level ϕ, $\frac{dq}{dN}(\phi = 0, \Delta K)$ is the fatigue crack growth rate at stress intensity factor range of ΔK of non-porous plate.

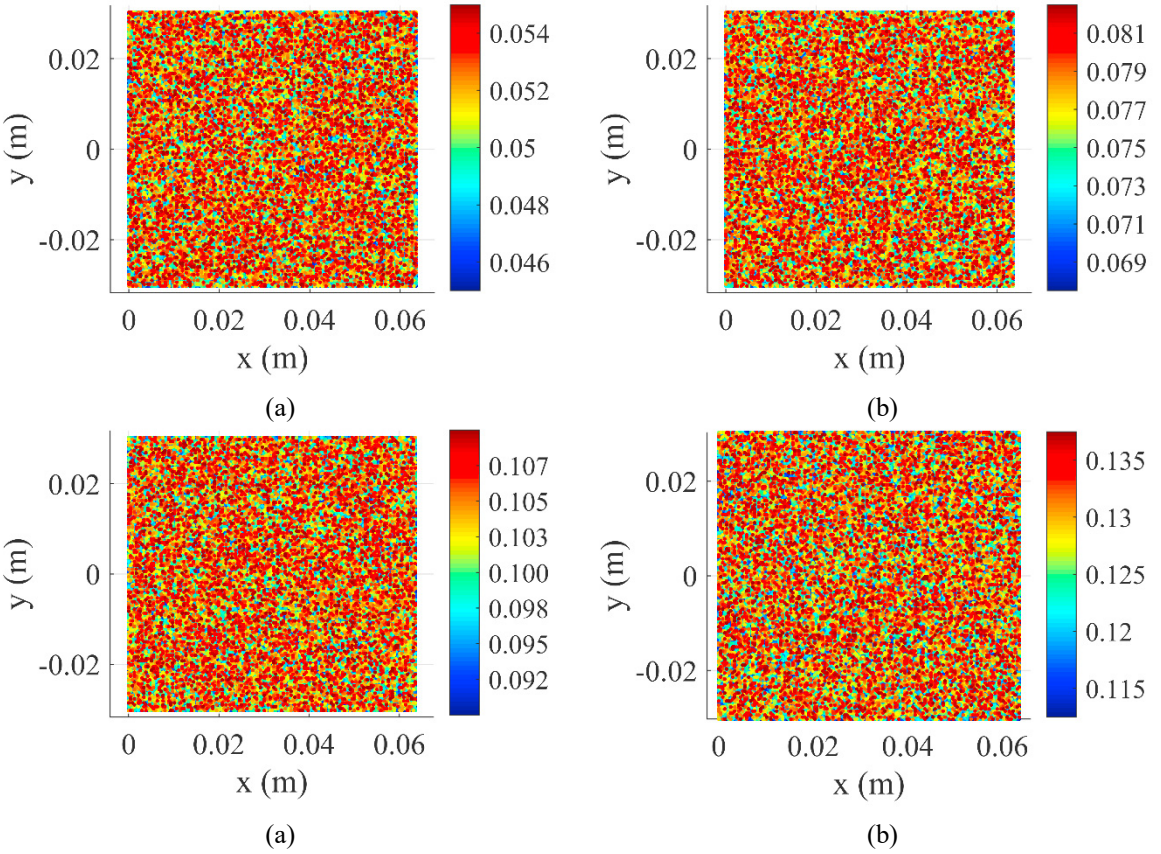

Fig. 4. Variation of local porosities on plates with average porosity levels of (a) $\phi_0 = 0.05$ (b) $\phi_0 = 0.075$, (c) $\phi_0 = 0.1$, (d) $\phi_0 = 0.125$

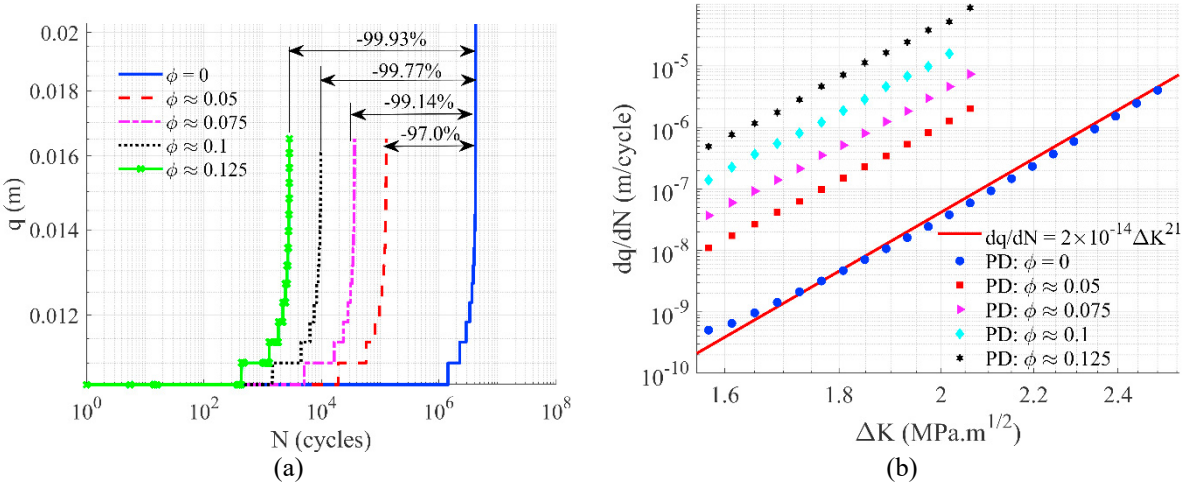

Fig. 5. Predicted fatigue crack growth (a) $q - N$ curves (b) $dq/dN - \Delta K$ curves for porous ceramic plates

By conducting a regression analysis, a linear relationship between $\overline{dq/dN}$, ϕ and ΔK is obtained with maximum error less than 6% as

$$\frac{\overline{dq}}{dN}(\phi, \Delta K) = 2.65579452\phi + 0.7639591\Delta K - 0.1414579 \quad (9)$$

4. Conclusion

In this study, fatigue crack growth in a ceramic material with different porosity levels is predicted by using the peridynamic fatigue model. The predicted fatigue crack growth rate of non-porous ceramic material agrees very well with experimental results. The influence of porosities on fatigue crack rate is also predicted. It is found that with porosity level of 0.05, the fatigue life of material is reduced 97%. Meanwhile, with porosity level of 0.125, the fatigue life of material is reduced 99.93%. Moreover, a linear relation between the relative change of fatigue crack growth rate, stress intensity factor range and porosity level is obtained by using linear regression analysis with the maximum error less than 6%.

Acknowledgements

This work was supported by an Institutional Links grant, ID 527426826, under the Egypt-Newton-Mosharafa Fund partnership. The grant is funded by the UK Department for Business, Energy and Industrial Strategy and Science, Technology and Innovation Funding Authority (STIFA) - project NO. 42717 (An Integrated Smart System of Ultrafiltration, Photocatalysis, Thermal Desalination for Wastewater Treatment) and delivered by the British Council. Results were obtained using the ARCHIE-WeSt High-Performance Computer (www.archie-west.ac.uk) based at the University of Strathclyde.

References

Dauskarat, R. H., Marshall, D. B., et al. 1990. Cyclic fatigue-crack propagation in magnesia-partially-stabilized zirconia ceramics. *Journal of the American ceramic society,* 73**,** 893-903.

Jung, J. & Seok, J. 2017. Mixed-mode fatigue crack growth analysis using peridynamic approach. *International Journal of Fatigue,* 103**,** 591-603.

Madenci, E. & Oterkus, E. 2014. *Peridynamic Theory and Its Applications,* New York, Springer.

Madenci, E. & Oterkus, S. 2016. Ordinary state-based peridynamics for plastic deformation according to von Mises yield criteria with isotropic hardening. *Journal of the Mechanics Physics of Solids,* 86**,** 192-219.

Nguyen, C. T., Oterkus, S., et al. 2020. An energy-based peridynamic model for fatigue cracking. *Engineering Fracture Mechanics,* 241**,** 107373.

Nguyen, C. T., Oterkus, S., et al. 2021. Implementation of Modified Wheeler Model in Peridynamic Fatigue Model to Predict Effects of Overload and Underload on Fatigue Crack Growth Rate. *Theoretical and Applied Fracture Mechanics***,** 103115.

Silling, S. A. 2000. Reformulation of elasticity theory for discontinuities and long-range forces. *Journal of the Mechanics and Physics of Solids,* 48**,** 175-209.

Silling, S. A. & Askari, A. 2014. Peridynamic model for fatigue cracking. *SAND-18590. Albuquerque: Sandia National Laboratories*.

Silling, S. A. & Askari, E. 2005. A meshfree method based on the peridynamic model of solid mechanics. *Computers & structures,* 83**,** 1526-1535.

Zhang, G., Le, Q., et al. 2016. Validation of a peridynamic model for fatigue cracking. *Engineering Fracture Mechanics,* 162**,** 76-94.